

Appendix 1. Full results of each scenario calculated following the method of Figure 2. Scenarios are detailed in Table S1.

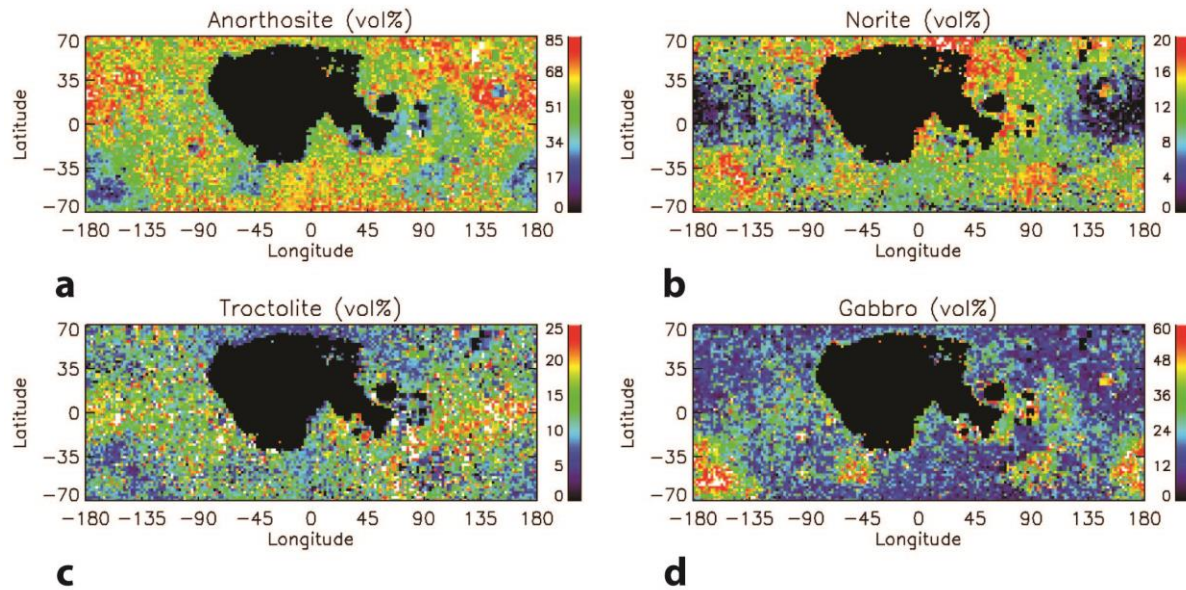


Figure S1. a-d) Rock type abundances calculated assuming pure anorthite and assigning all excess mafics to post-magma ocean igneous products.

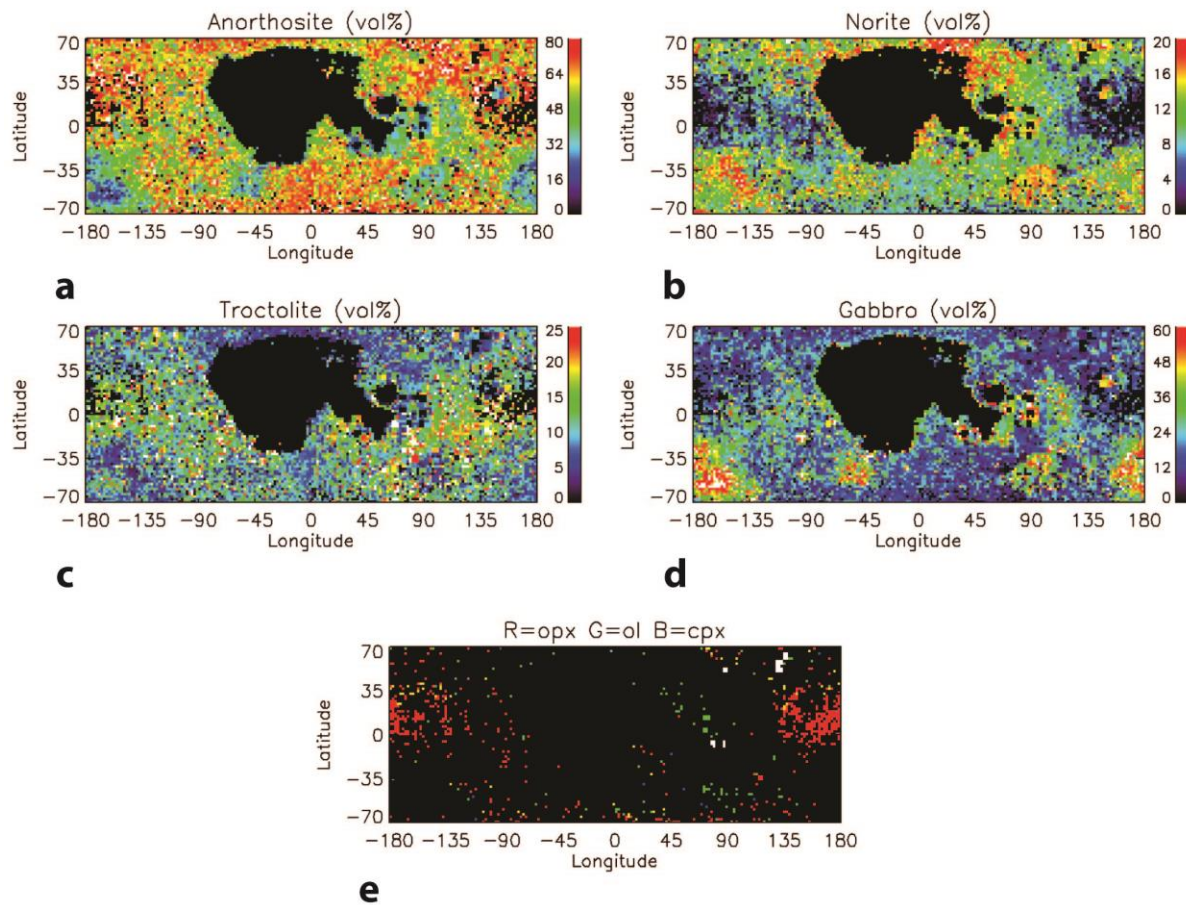


Figure S2. a-d) Rock type abundances calculated assuming PAN (2 vol% mafics) and assigning all excess mafics to post-magma ocean igneous products. e) Map showing the limiting mafic minerals at “no solution” pixels for anorthosites of the assumed mafic abundance and composition.

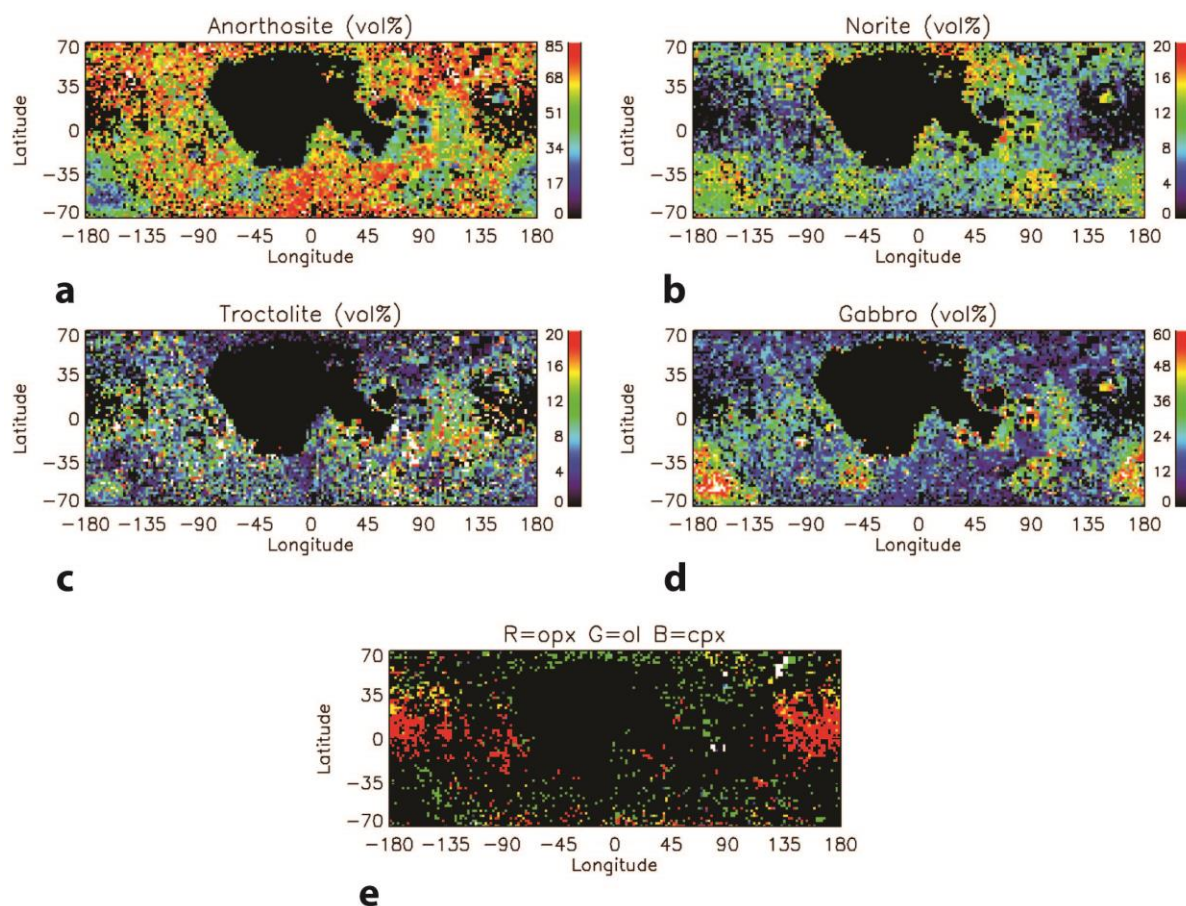


Figure S3. a-d) Rock type abundances calculated assuming 7 vol% mafics and assigning all excess mafics to post-magma ocean igneous products. e) Map showing the limiting mafic minerals at “no solution” pixels for anorthosites of the assumed mafic abundance and composition.



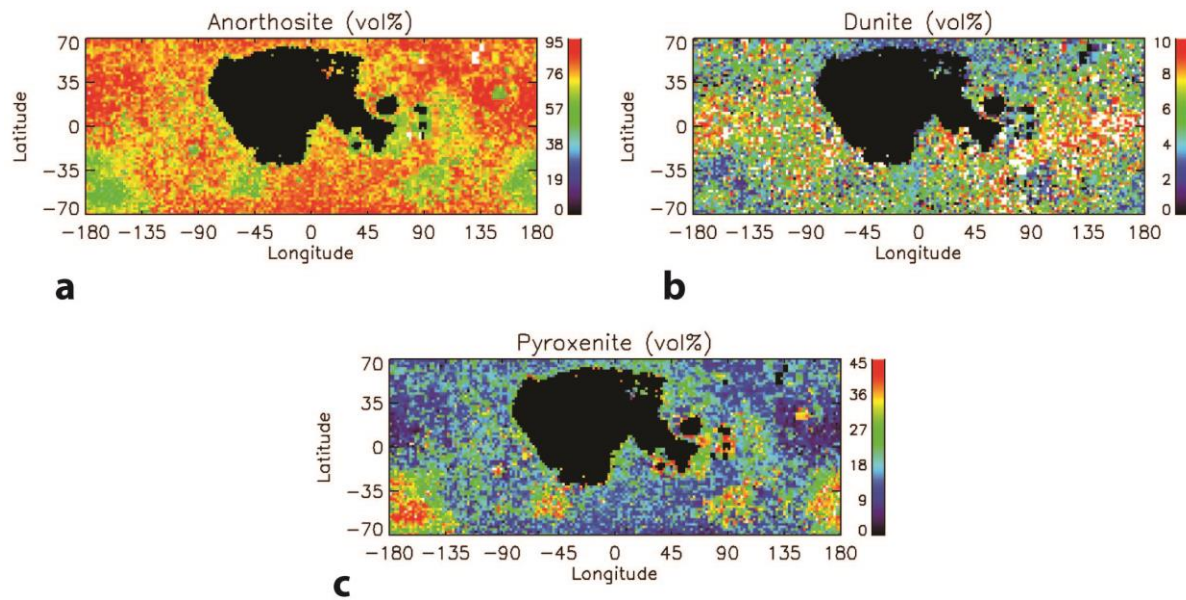


Figure S4. a-c) Rock type abundances calculated assuming pure anorthite and assigning all excess mafics to mantle rocks (dunite and pyroxenite). Pixels where both are present are also consistent with peridotite.

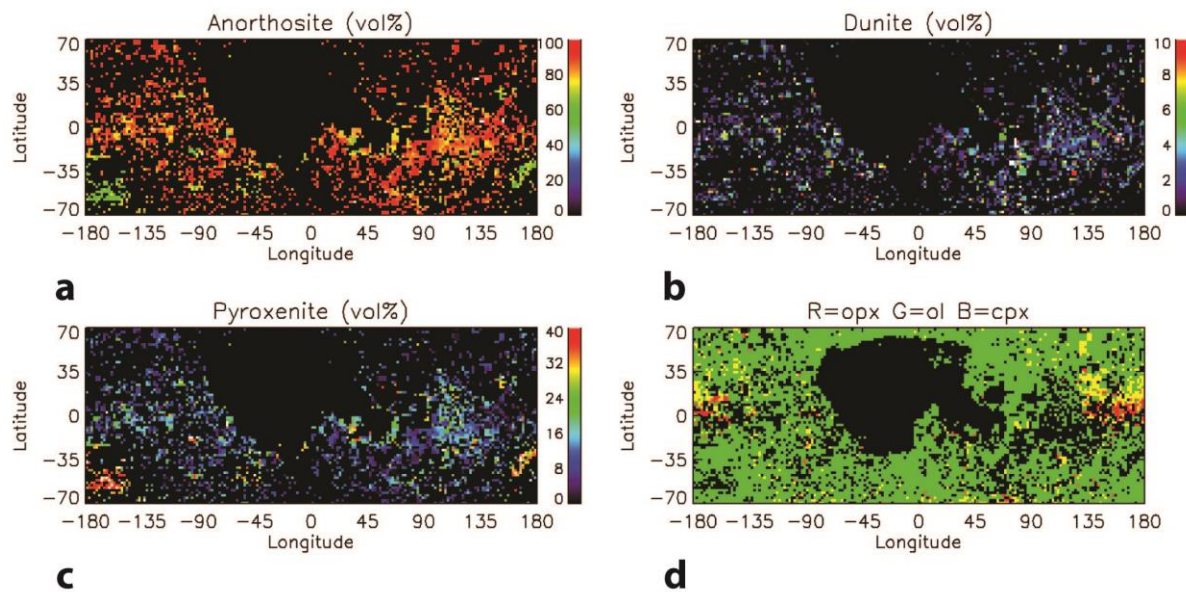


Figure S5. a-c) Rock type abundances calculated assuming 15 vol% mafics and assigning all excess mafics to mantle rocks (dunite and pyroxenite). Pixels where both are present are also consistent with peridotite. d) Map showing the limiting mafic minerals at “no solution” pixels for anorthosites of the assumed mafic abundance and composition.

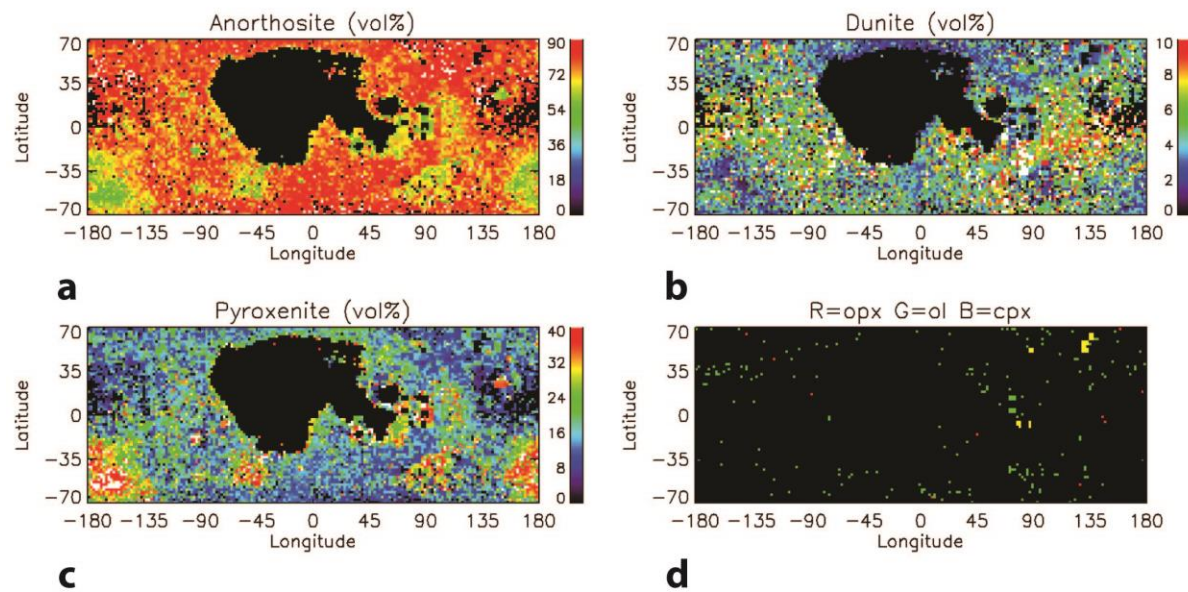


Figure S6. a-c) Rock type abundances calculated assuming PAN (2 vol% mafics) and assigning all excess mafics to mantle rocks (dunite and pyroxenite). Pixels where both are present are also consistent with peridotite. d) Map showing the limiting mafic minerals at “no solution” pixels for anorthosites of the assumed mafic abundance and composition.

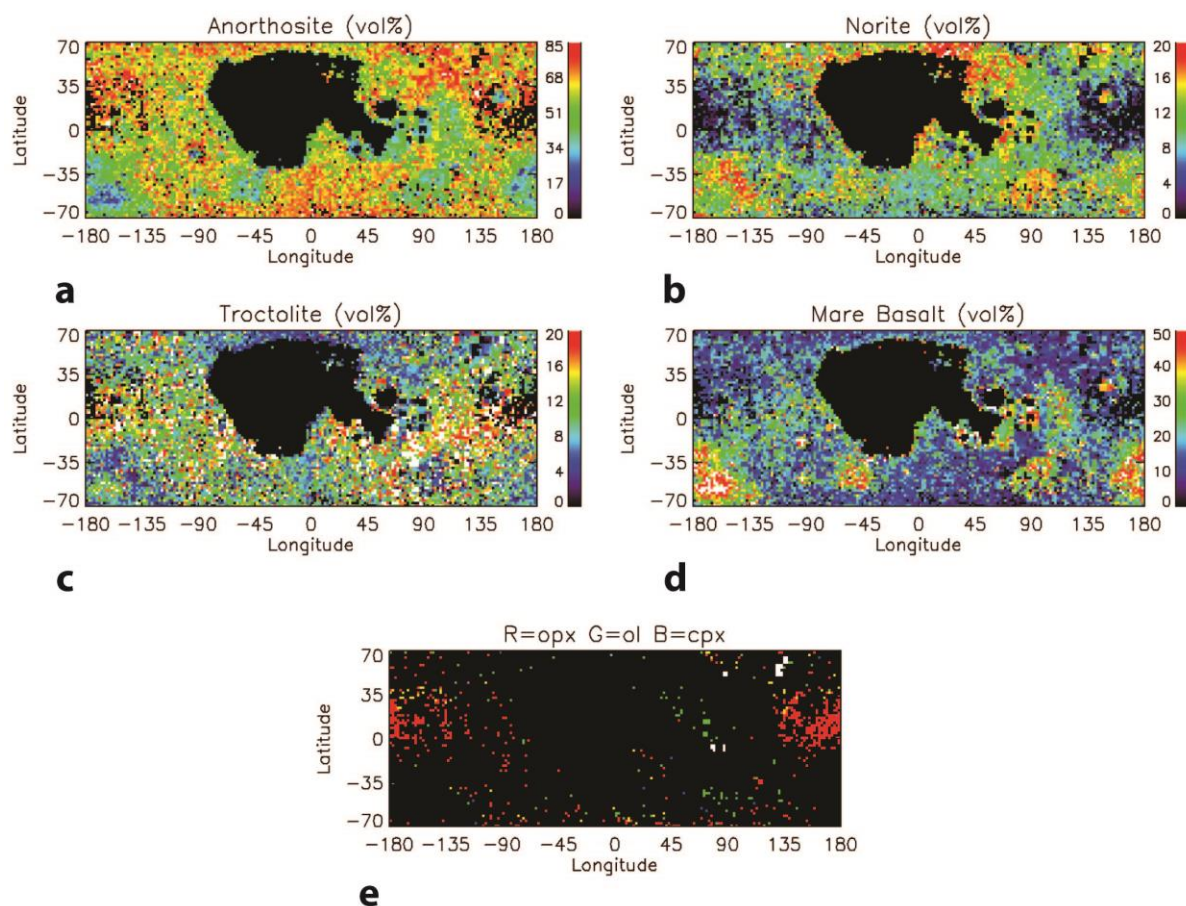


Figure S7. a-d) Rock type abundances calculated assuming PAN (2 vol% mafics) and assigning all excess mafics to post-magma ocean igneous material, with clinopyroxene assumed to be present in the form of mare basalt. e) Map showing the limiting mafic minerals at “no solution” pixels for anorthosites of the assumed mafic abundance and composition.



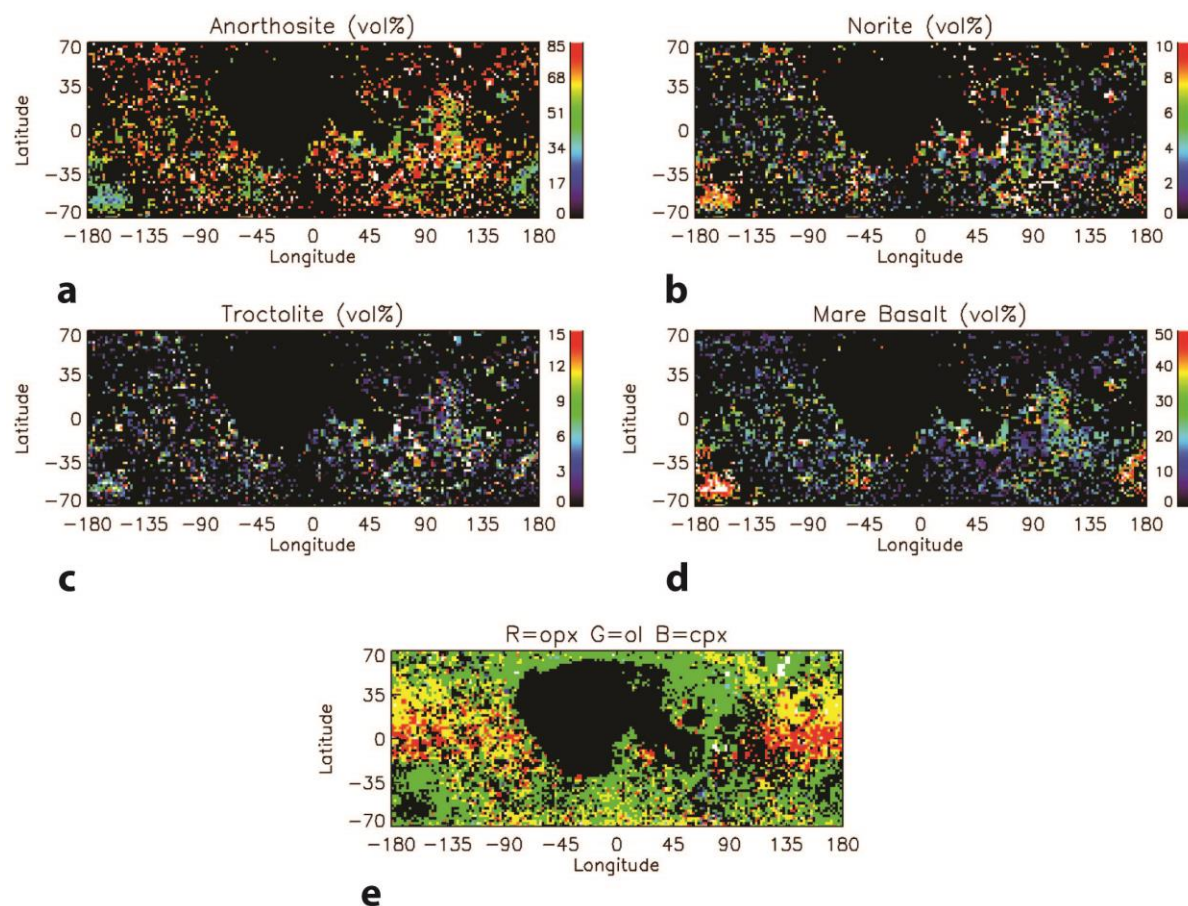


Figure S8. a-d) Rock type abundances calculated assuming 15 vol% mafics and assigning all excess mafics to post-magma ocean igneous material, with clinopyroxene assumed to be present in the form of mare basalt. e) Map showing the limiting mafic minerals at “no solution” pixels for anorthosites of the assumed mafic abundance and composition.

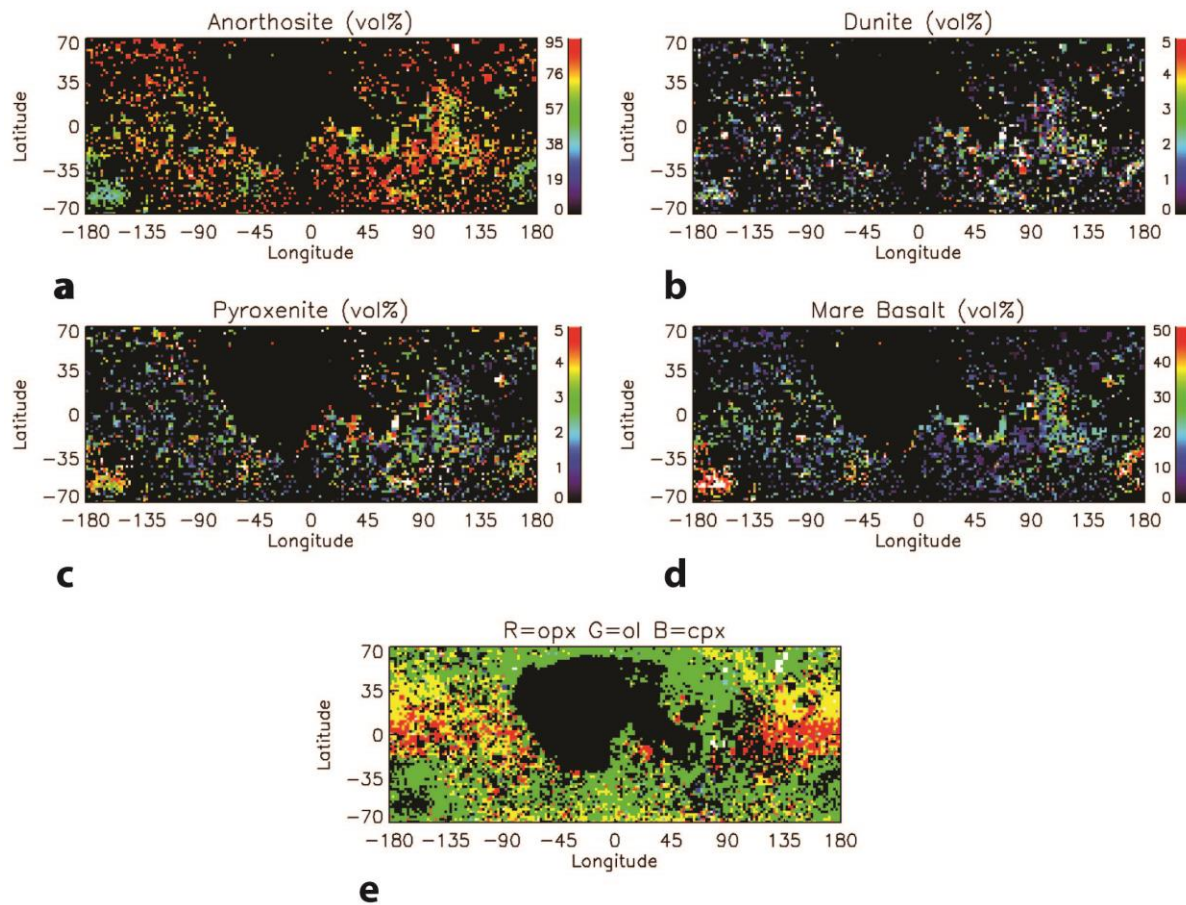


Figure S9. a-d) Rock type abundances calculated assuming 15 vol% mafics and assigning all excess orthopyroxene and olivine to mantle rocks (dunite and pyroxenite). Pixels where both are present are also consistent with peridotite. All clinopyroxene was assigned to mare basalt. e) Map showing the limiting mafic minerals at “no solution” pixels for anorthosites of the assumed mafic abundance and composition.



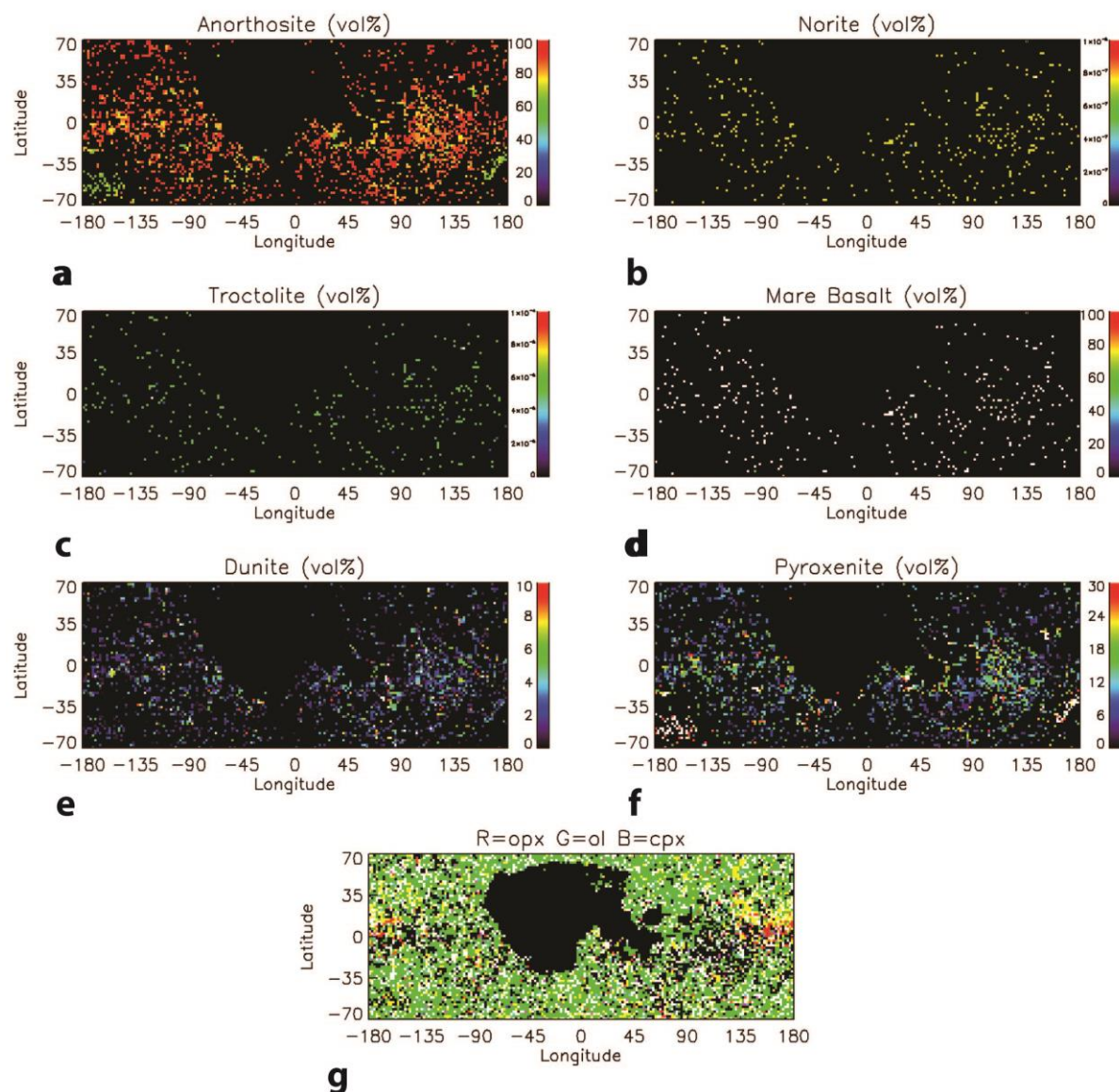


Figure S10. a-f) Rock type abundances calculated assuming 15 vol% mafics and assigning mafics to mantle rocks (dunite and pyroxenite) up to an upper limit of 40 vol%, with mafics above this limit assigned to post-magma ocean igneous products. Pixels where both dunite and pyroxenite are present are also consistent with peridotite. g) Map showing the limiting mafic minerals at “no solution” pixels for anorthosites of the assumed mafic abundance and composition.

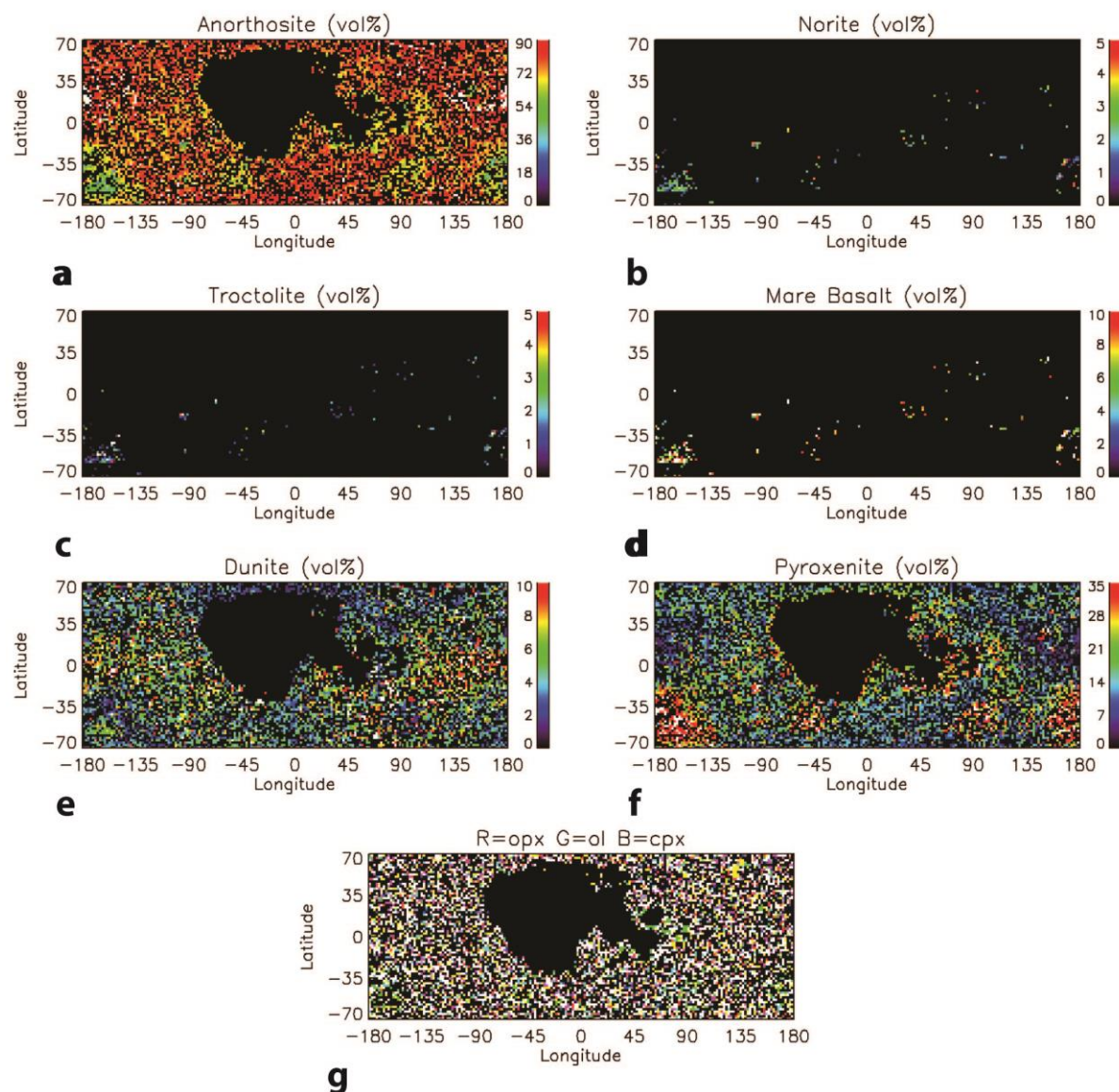


Figure S11. a-f) Rock type abundances calculated assuming PAN (2 vol% mafics) and assigning mafics to mantle rocks (dunite and pyroxenite) up to an upper limit of 40 vol%, with mafics above this limit assigned to post-magma ocean igneous products. Pixels where both dunite and pyroxenite are present are also consistent with peridotite. g) Map showing the limiting mafic minerals at “no solution” pixels for anorthosites of the assumed mafic abundance and composition.

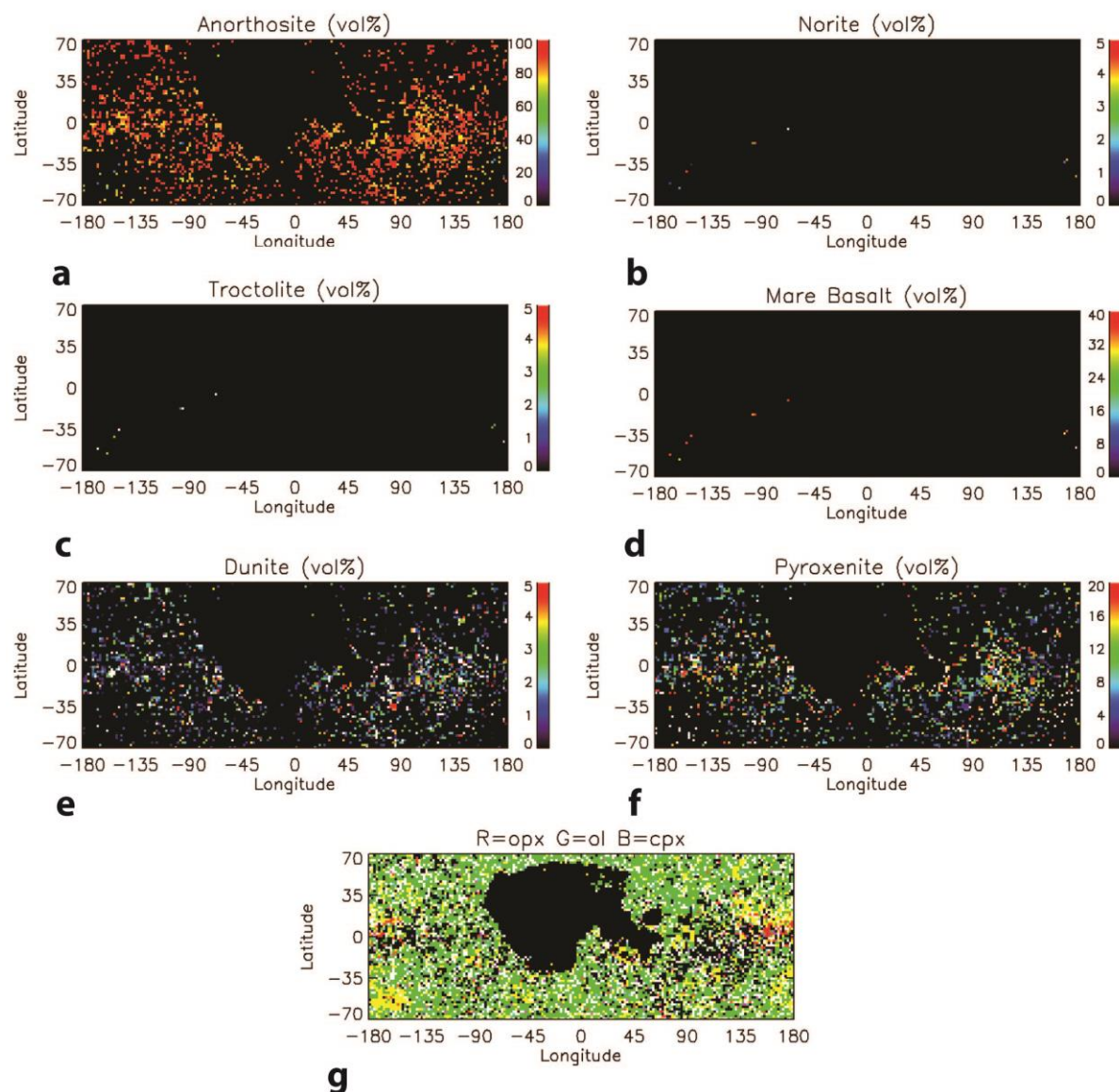


Figure S12. a-f) Rock type abundances calculated assuming 15 vol% mafics and assigning mafics to mantle rocks (dunite and pyroxenite) up to an upper limit of 30 vol%, with mafics above this limit assigned to post-magma ocean igneous products. Pixels where both dunite and pyroxenite are present are also consistent with peridotite. g) Map showing the limiting mafic minerals at “no solution” pixels for anorthosites of the assumed mafic abundance and composition.



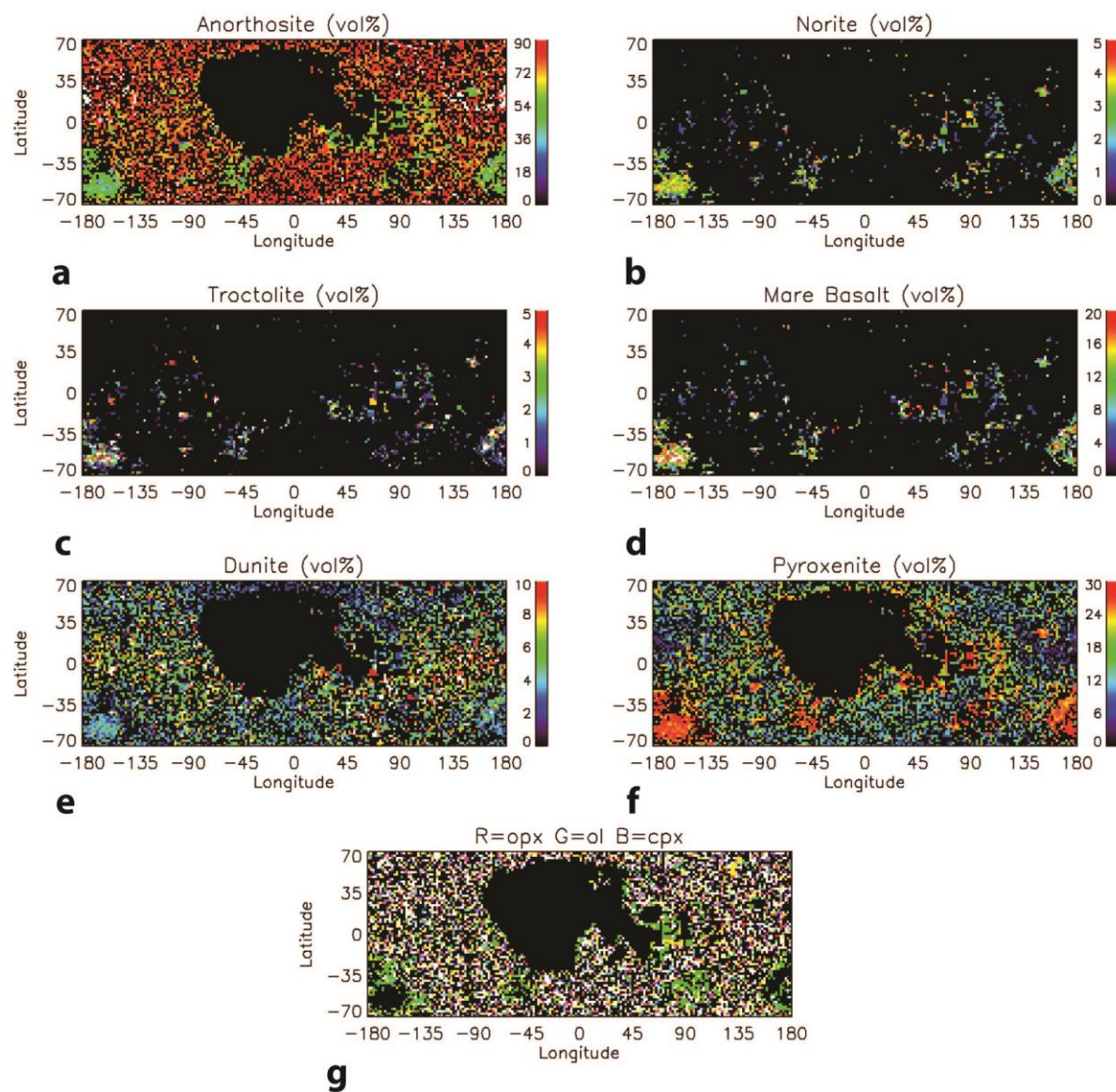


Figure S13. a-f) Rock type abundances calculated assuming PAN (2 vol% mafics) and assigning mafics to mantle rocks (dunite and pyroxenite) up to an upper limit of 30 vol%, with mafics above this limit assigned to post-magma ocean igneous products. Pixels where both dunite and pyroxenite are present are also consistent with peridotite. g) Map showing the limiting mafic minerals at “no solution” pixels for anorthosites of the assumed mafic abundance and composition.

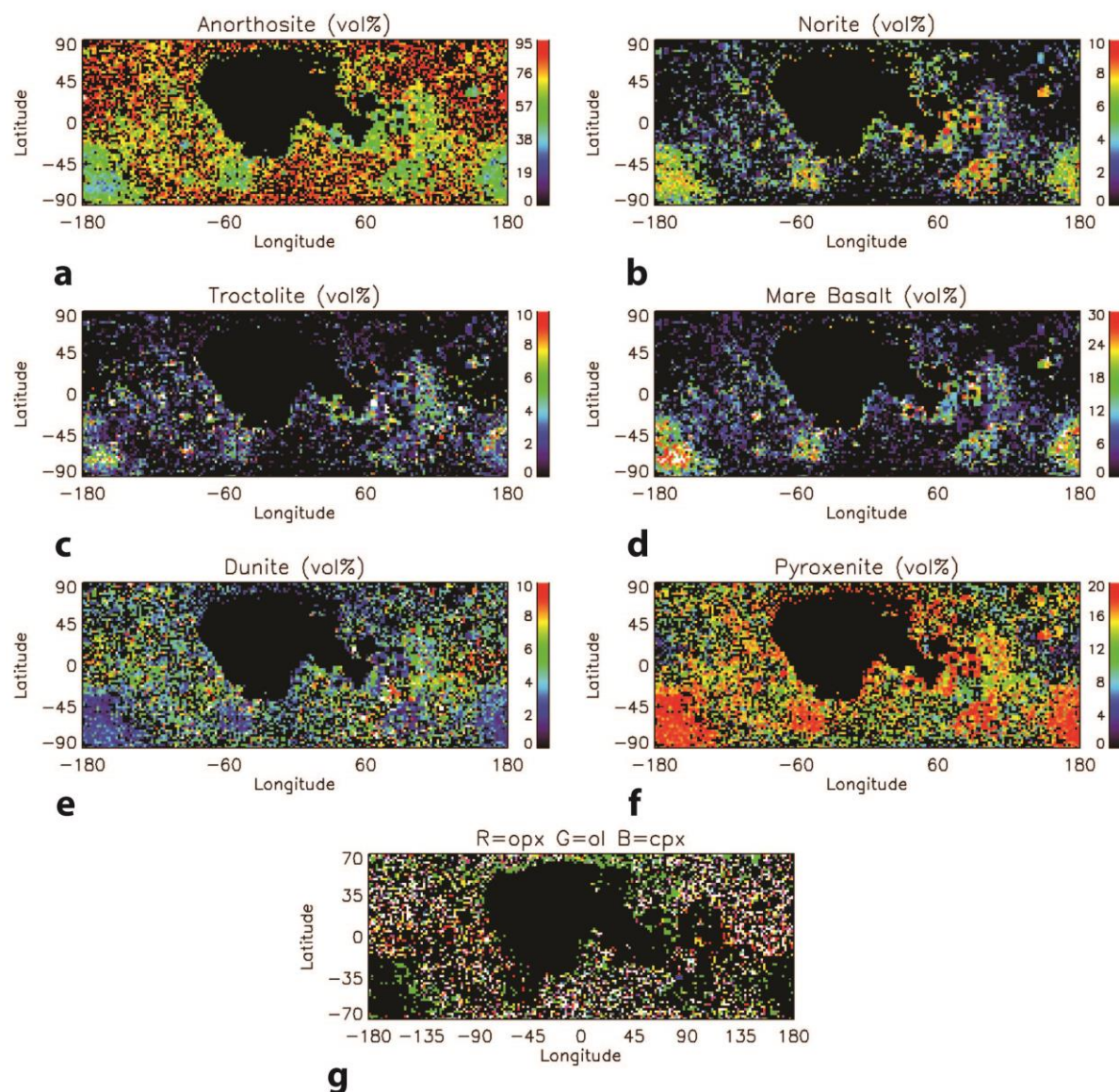


Figure S14. a-f) Rock type abundances calculated assuming PAN (2 vol% mafics) and assigning mafics to mantle rocks (dunite and pyroxenite) up to an upper limit of 20 vol%, with mafics above this limit assigned to post-magma ocean igneous products. Pixels where both dunite and pyroxenite are present are also consistent with peridotite. g) Map showing the limiting mafic minerals at “no solution” pixels for anorthosites of the assumed mafic abundance and composition.



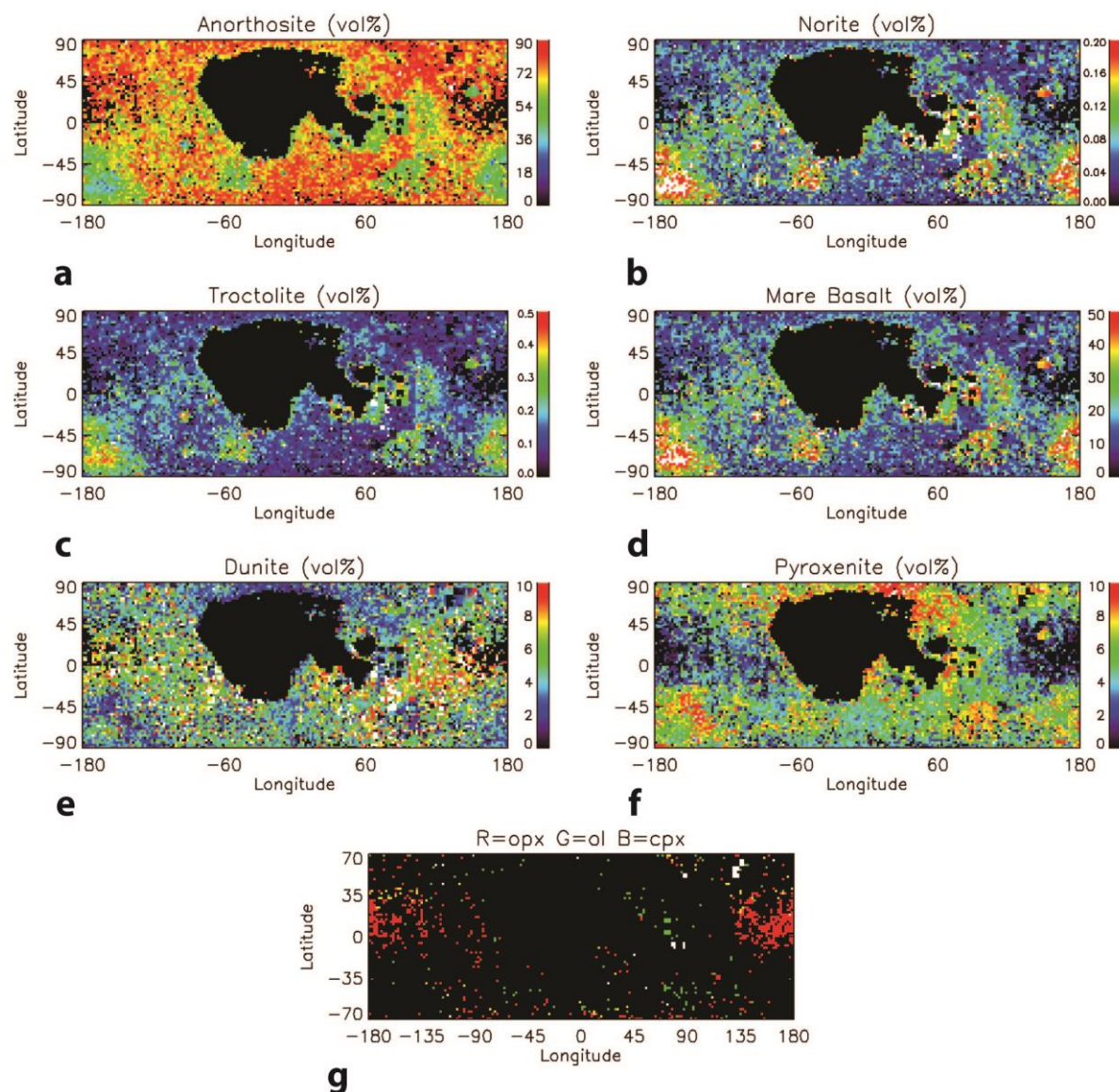


Figure S15. a-f) Rock type abundances calculated assuming PAN (2 vol% mafics) and assigning olivine and orthopyroxene to mantle rocks (dunite and pyroxenite) up to an upper limit of 20 vol%, with mafics above this limit assigned to post-magma ocean igneous products. All clinopyroxene was assumed to be present in the form of mare basalt. Pixels where both dunite and pyroxenite are present are also consistent with peridotite. g) Map showing the limiting mafic minerals at “no solution” pixels for anorthosites of the assumed mafic abundance and composition.



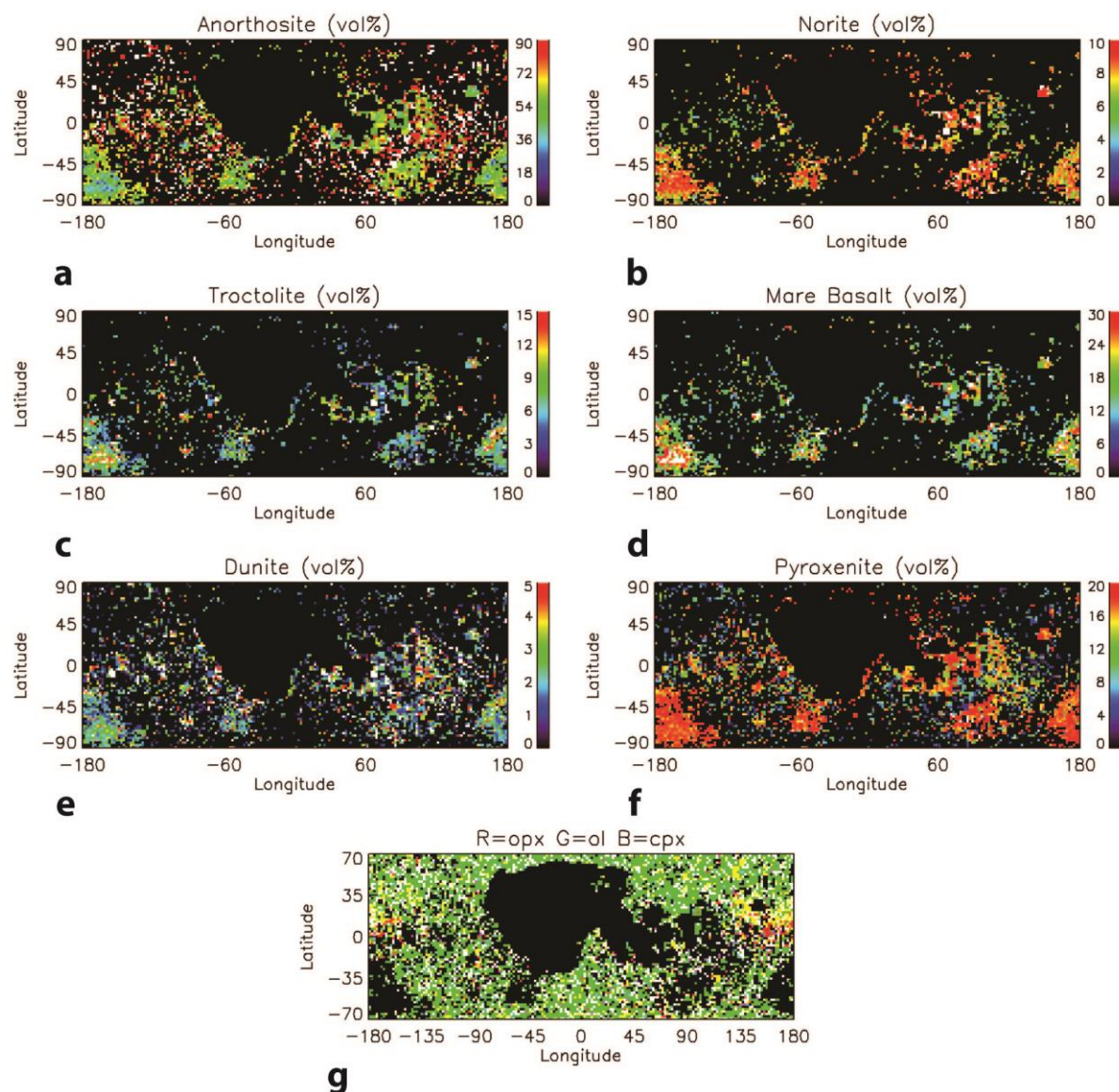


Figure S16. a-f) Rock type abundances calculated assuming 15 vol% mafics and assigning mafics to mantle rocks (dunite and pyroxenite) up to an upper limit of 20 vol%, with mafics above this limit assigned to post-magma ocean igneous products. Pixels where both dunite and pyroxenite are present are also consistent with peridotite. g) Map showing the limiting mafic minerals at “no solution” pixels for anorthosites of the assumed mafic abundance and composition.

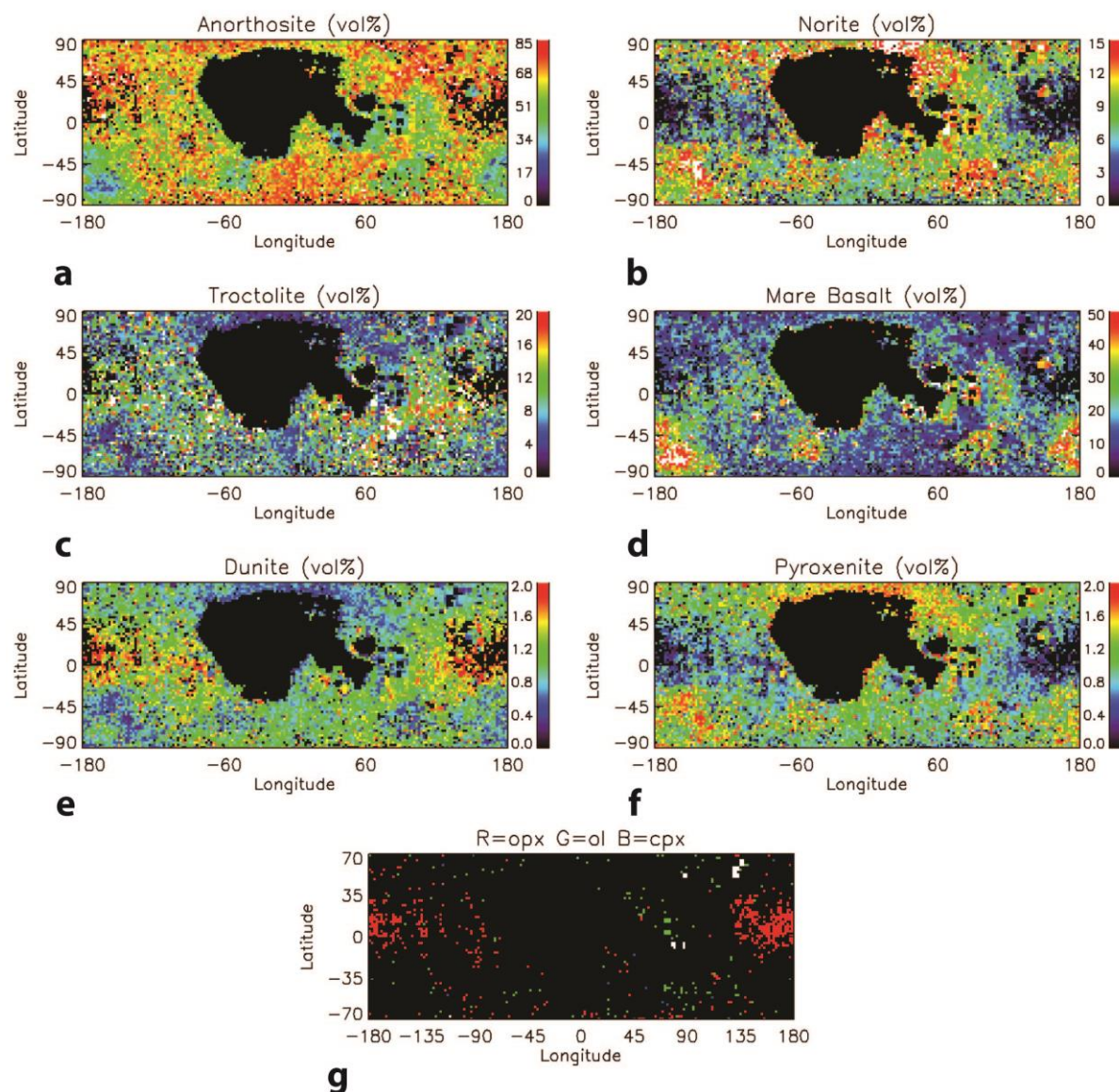


Figure S17. a-f) Rock type abundances calculated assuming PAN (2 vol% mafics) and assigning olivine and orthopyroxene to mantle rocks (dunite and pyroxenite) up to an upper limit of 2 vol%, with mafics above this limit assigned to post-magma ocean igneous products. All clinopyroxene was assumed to be present in the form of mare basalt. Pixels where both dunite and pyroxenite are present are also consistent with peridotite. g) Map showing the limiting mafic minerals at “no solution” pixels for anorthosites of the assumed mafic abundance and composition.



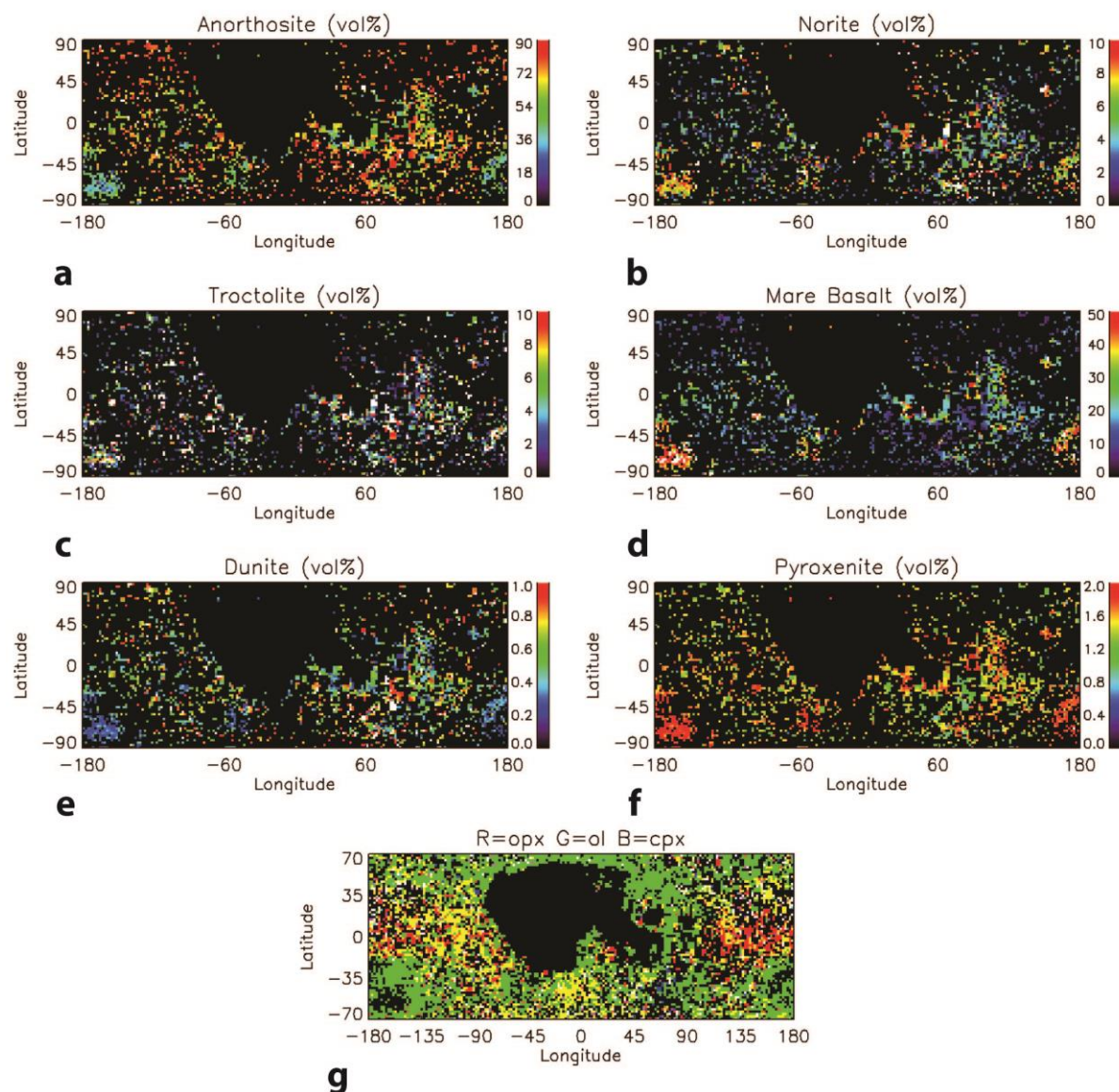


Figure S18. a-f) Rock type abundances calculated assuming 15 vol% mafics and assigning mafics to mantle rocks (dunite and pyroxenite) up to an upper limit of 2 vol%, with mafics above this limit assigned to post-magma ocean igneous products. Pixels where both dunite and pyroxenite are present are also consistent with peridotite. g) Map showing the limiting mafic minerals at "no solution" pixels for anorthosites of the assumed mafic abundance and composition.